ICARUS report to the 126th Meeting of SPSC, June 20-21, 2017

Table of content

1 The ICARUS Collaboration

M. Antonello[a], B. Baibussinov[b], V. Bellini[p], P. Benetti[c], F. Boffelli[c], A. Bubak[k], E. Calligarich[c], S. Centro[b], A. Cesana[f], K. Cieslik[g], A.G. Cocco[d], A. Dabrowska[g], A. Dermenev[i], A. Falcone[c] , C. Farnese[b], A. Fava[b], A. Ferrari[j], D. Gibin[b], S. Gninenko[i], A. Guglielmi[b], M. Haranczyk[g], J. Holeczek[k], M. Janik[k], M. Kirsanov[i], J. Kisiel[k], I. Kochanek[k], J. Lagoda[l], S. Mania[k], A. Menegolli[c], G. Meng[b], C. Montanari[c,j], S. Otwinowski[h], P. Picchi[m], F. Pietropaolo[b,j], P. Plonski[n], A. Rappoldi[c], G.L. Raselli[c], M. Rossella[c], C. Rubbia[a,j,q], P. Sala[f,j], A. Scaramelli[f], F. Sergiampietri[o], D. Stefan[f], R. Sulej[l], M. Szarska[g], M. Terrani[f], M. Torti[c], F. Tortorici [p], F. Varanini[b], S. Ventura[b], C. Vignoli[a], H. Wang[h], X. Yang[h], A. Zalewska[g], A. Zani[c], K. Zaremba[n].

a Laboratori Nazionali del Gran Sasso dell'INFN, Assergi (AQ), Italy
b Dipartimento di Fisica e Astronomia e INFN, Università di Padova, Via Marzolo 8, I-35131 Padova, Italy
c Dipartimento di Fisica Nucleare e Teorica e INFN, Università di Pavia, Via Bassi 6, I-27100 Pavia, Italy
d Dipartimento di Scienze Fisiche, INFN e Università Federico II, Napoli, Italy
f INFN, Sezionedi Milano e Politecnico, Via Celoria16, I-20133 Milano, Italy
g Henryk Niewodniczanski Institute of Nuclear Physics, Polish Academy of Science, Krakow, Poland
h Department of Physics and Astronomy, University of California, Los Angeles, USA
i INR RAS, prospect 60-letiya Oktyabrya 7a, Moscow 117312, Russia
j CERN, CH-1211 Geneve 23, Switzerland
k Institute of Physics, University of Silesia, 4 Uniwersytecka st., 40-007 Katowice, Poland
l National Centre for Nuclear Research, 05-400 Otwock/Swierk, Poland
m Laboratori Nazionali di Frascati (INFN), Via Fermi 40, I-00044 Frascati, Italy
n Institute of Radioelectronics, Warsaw University of Technology, Nowowiejska, 00665 Warsaw, Poland
o INFN, Sezione di Pisa. Largo B. Pontecorvo, 3, I-56127 Pisa, Italy
p Dipartimento di Fisica Astronomia e INFN, Università di Catania, via S. Sofia 64, I-95123 Catania, Italy
q GSSI, Gran Sasso Science Institute, L'Aquila, Italy.

2 Introduction

The Cherenkov radiation detection has been so far one of the key choices for exploring the particle physics frontier with tens kt mass water and ice detectors to study the neutrino interactions at accelerators and the atmospheric and solar neutrinos and to search for rare events like Super-Novae explosions and nucleon decay. Unfortunately, these detectors do not permit to identify unambiguously each ionizing track produced in the complex neutrino interactions.

As an alternative, the Liquid Argon (LAr) Time Projection Chamber (TPC) technology, based on the drift of electrons produced by any ionizing particle in pure LAr by an electric field, was proposed in 1977 by C. Rubbia [1]. This novel detector allows for (1) three-dimensional track reconstruction and (2) calorimetric measurement. Due to these two features the LAr-TPC can be considered as a continuously sensitive electronic bubble chamber which, contrary to traditional bubble chambers, can be scaled to larger masses to be successfully employed to register rare events like neutrino interactions and to search for the nucleon decay.

The LAr-TPC detection technique has been taken to the full maturity with the realization of the ICARUS-T600 (see Section 2), the biggest Liquid Argon detector ever realized containing 760 t (460 t of active mass), which was installed and operated in the underground Gran Sasso Laboratory (LNGS). It is a result of many years of R&D studies performed by the ICARUS Collaboration with the continuous support of INFN aiming to realize laboratory and industrial prototypes of growing mass culminating with the first observation of a CNGS neutrino interaction in ICARUS T600 LAr-TPC in May 2010.

ICARUS-T600 completed in 2013 a successful continuous three years run at LNGS, being exposed to both CNGS neutrino beam and cosmic rays. During the LNGS operation, ICARUS obtained many different technical and physical achievements proving the validity of the LAr-TPC technology (see the *List of selected ICARUS publications*).

The ICARUS cryogenic plant permitted smooth and safe operations under stable running conditions in a difficult underground environment like the LNGS as described in Section 3. The adopted argon recirculation and purification system permitted to reach an impressive LAr purity, with less than 20 parts per trillion of oxygen-equivalent contamination, corresponding to an extremely high free electron lifetime exceeding 16 ms. This result represents a milestone for the all future LAr-TPC projects involving much higher volumes and larger electron drift paths.

The special designed trigger system based on the scintillation light detection and complemented with the charge signal detection on the TPC wires (see Section 4), allowed to collect with high efficiency ~3000 CNGS neutrino interactions and a large sample of cosmic events.

The recorded events demonstrated the excellent detection performance of ICARUS as a tracking device and as a homogeneous calorimeter. Section 5 deals with three-dimensional reconstruction of ionizing events, permitted by the combination of the information from the different wire planes. Moreover, remarkable particle identification capabilities have been determined exploiting the measurement of dE/dx vs. range. The abilities to reconstruct the neutrino interaction vertex within a very broad energy range and complex event topologies, combined with identification and measurement of e.m. showers generated by primary electrons and with accurate measurement of the invariant mass of photon pairs, allowed to reject the backgrounds in the study of $\nu\mu \rightarrow \nu e$ transitions at an unprecedented level. The multiple Coulomb scattering method adopted to measure muon momenta (up to ~5 GeV/c) in LAr-TPC was validated with stopping muons from the interactions of CNGS neutrinos in the upstream rock (see Section 6).

The collected data allowed studying with high accuracy both the CNGS ν_μCC and ν_e CC interactions and the atmospheric neutrino events. ICARUS performed a sensitive search for a potential νe excess related to LSND-like anomalies in the high energy CNGS ν_μ beam (Section 7). The favored explanation of the longstanding LNSD experiment anomaly, together with the other experimental hints of apparent disappearance in reactor anti-νe and solar neutrino calibration sources, involves the existence of new sterile neutrino flavors with additional larger mass-squared differences. The ICARUS study permitted to define a much smaller, narrower region for $\Delta m^2 \leq 1$ eV^{2}eV^2 in which there is 90 % CL agreement between (1) the present ICARUS and OPERA limits, (2) the limits of KARMEN and (3) the positive signals of LSND and MiniBooNE collaborations. Soon after the 2011 surprising claim of super-luminal

neutrinos by the OPERA experiment with the CNGS neutrino beam, ICARUS proved, both indirectly and by direct t.o.f. measurement, that neutrino do not propagate faster than light (see section 8).

All these results mark a milestone for the LAr-TPC technology with a large impact on the future neutrino and astro-particle physics projects, like the current FNAL short-baseline neutrino (SBN) program with three LAr-TPC detectors (SBND, MicroBooNE and ICARUS-T600), and the considered multi-kt DUNE LAr-TPC detector.

Presently at CERN for an extensive overhauling, the ICARUS-T600 detector will be soon transported to FNAL and exposed to the 0.8 GeV FNAL Booster neutrino beam at 600 m from the target. The comparison of the ν spectra measured by ICARUS with those measured by SBND and MicroBooNE at 110 and 470 m from target respectively will allow to finally prove or discard the hints for a new ``sterile'' neutrino state as indicated by LSND (Section 12). In absence of "anomalies", the spectra will be a precise copy of each other, without the need of any Monte Carlo (MC) comparison. ICARUS will also collect a large sample of νe CC events from the NUMI off-Axis beam at ~ 2 GeV which will provide valuable information for the future DUNE project.

3 The ICARUS T600 detector

The ICARUS T600 consists of a large cryostat split into two identical, adjacent half-modules with internal dimensions 3.6 x 3.9 x 19.6 m^3 and filled with 760 tons of ultra-pure liquid Argon (LAr) [P5][P11], see Figure 1.

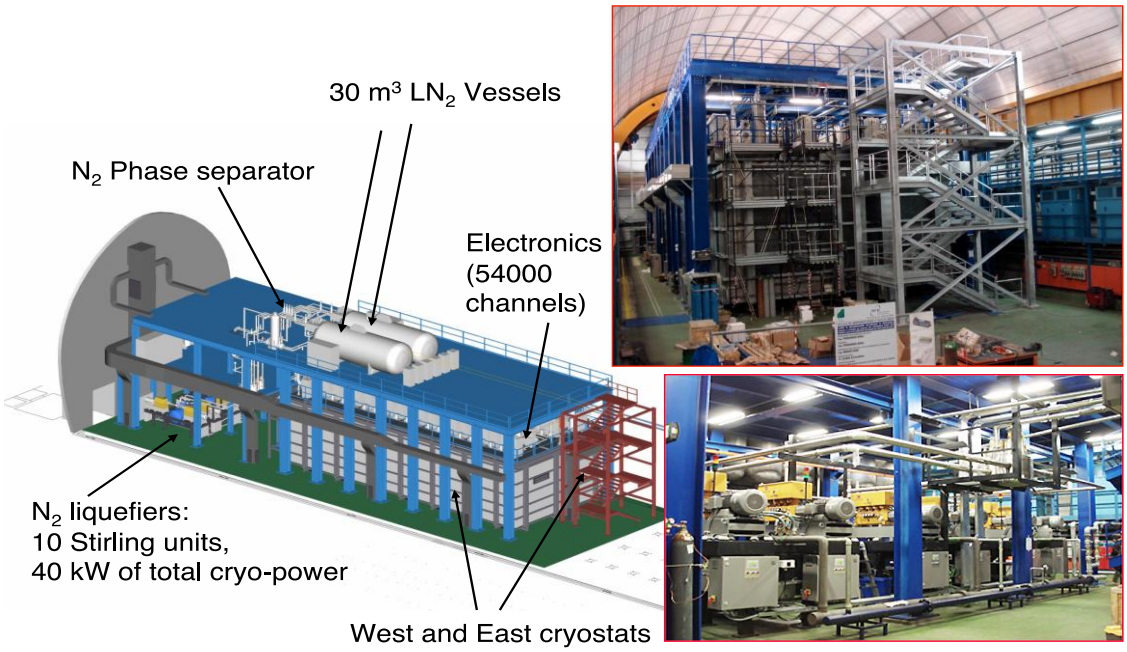

Figure 1. Left: Schematic view of the whole ICARUS T600 plant in Hall-B at LNGS. Right-top: photo of the actual detector installation. Right-bottom: details of the cryo-coolers plant.

Each half-module houses two Time Projection Chambers (TPC) separated by a common cathode, a field shaping system, two arrays of photo-multiplier tubes (PMT), monitors and probes.

Charged particles crossing LAr copiously produce ionization electrons which are drifted undistorted by a uniform 500 V/cm electric field to the three parallel wire-planes, 3 mm apart, facing the drift region, with wires oriented at 0°and ±60° with respect to the horizontal direction. Globally, 53248 wires with length up to 9 m are installed in the detector. By appropriate voltage biasing, the first two planes (Induction 1 and Induction 2) provide signals in non-destructive way, whereas the charge is finally collected in the last one (Collection). The maximum drift path, i.e. the distance between the cathode and the wire planes, is 1.5 m. The signals coming from each wire are independently digitized every 400 ns resulting in a ~1 mm^3 spatial resolution.

The measurement of the absolute time of the ionizing event, which can be determined via the prompt scintillation light (λ=128 nm) produced by charged particles in LAr, together with the knowledge of the electron drift velocity v_D ~ 1.6 mm/μs, provides the position of the tracks along the drift coordinate. For these purposes, a total of 74 (9357FLA Electron Tubes) PMT's with the glass windows coated with tetra-phenyl-butadiene wavelength shifter, are deployed in the LAr along three horizontal rows behind the wire planes of the TPCs.

The ICARUS electronics was designed to allow continuous read-out, digitization and independent waveform recording of signals from each wire of the TPC. The overall gain is ~1000 electrons per ADC count, setting the signal of minimum ionizing particles (m.i.p.) to ~ 15 ADC counts with a dynamic range of about 100 m.i.p. The average electronic noise was measured to be well within expectations: ~1600 electrons r.m.s. to be compared with ~15000 free electrons produced by m.i.p. in 3 mm (S/N ~ 9 in Collection).

Identification of protons, kaons, pions and muons is obtained through energy deposited per track length unit (dE/dx) versus particle range, and by studying the decay/interaction topology. Electrons are identified by their characteristic electromagnetic showering. They can be distinguished from π^0 at the level of per mil using dE/dx comparison of photon and electron in the first few wires, and π^0 mass reconstruction. The estimated σ(E)/E energy resolutions are: 3%/√E(GeV), 30%/√E(GeV) and 11%√E(GeV) + 2% for contained e.m. showers, hadronic showers and low energy electrons, respectively.

The smooth ICARUS operations under stable running conditions for more than three years at the nominal E=500 V/cm drift field without any failure allowed to take data with the CNGS beam with remarkable detector live-time > 93 %. Different operating conditions have been successfully tested in the last months of run proving that ICARUS can safely stand up to ~1 kV/cm drift electric field without any discharges (see Figure 2).

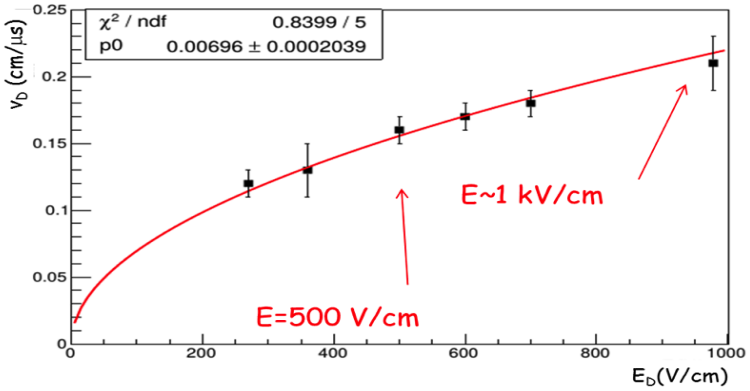

Figure 2: The electron drift velocity as a function of the electric drift field as measured with cosmic crossing both cathode and wire planes. The fit red line is in agreement with the dependence of v_D on $\sqrt{E_D}$.

4 Cryogenics systems and LAr purity

One of the main technological challenges in the LAr-TPC detector is the development of a cryogenic plant capable to cope with the demanding high liquid argon purity. The residual level of electronegative impurities, mainly O_2, has to be kept as low as 0.1 parts per billion (ppb) all over the argon volume to drift the electron ionization signal without significant attenuation to the TPC wire planes. The solutions developed by the ICARUS Collaboration over about 20 years of R&D to cope with argon purity specifications are essentially based on:

- The use of commercial argon filters operated directly in liquid phase: Hydrosorb™ for water removal and Oxysorb™ for oxygen removal;
- The adoption of ultra-high vacuum components (such as standard UHV CF flanges) and techniques for the detector construction;
- The commissioning procedures involving an initial vacuum phase to remove air and outgas all the internal surfaces followed by fast cryostat LN_2 cooling and LAr filling with purified argon;

- The continuous gas and liquid argon re-circulation system, both involving argon purification in liquid phase, to attain and maintain the required purity level.

The T600 cryogenic plant (see Figure 1) described in details in [P21] was characterized by high intrinsic modularity, redundancy and specific infrastructure for the three years long underground operation. The ICARUS T600 cryostat, designed in strict partnership with Air Liquide Italia Company, was composed by two identical adjacent aluminum LAr containers, with independent argon containment and purification plants but sharing the cooling shield (LAr thermal uniformity within 1 K in the LAr volume) and the insulation vessel. The T600 was first operated on surface in 2001 to validate the implemented solutions for the cryogenic plant and verify detector performance [P5]. Then the cryogenic plant was improved mainly for safety aspects connected with the underground operation and finally installed inside the Gran Sasso Laboratory [P7][P21]. The necessary cold power was supplied by a nitrogen re-liquefaction system working in closed loop and consisting of twelve cryo-coolers, based on the "reverse Stirling thermodynamic cycle", delivering 4.1 kW of cold power each at 84 K with an efficiency of 10.4% [17].

Each module was equipped with two GAr systems behaving as a precise and continuous pressure stabilizer, and one LAr re-circulation system. GAr re-condensed in a dedicated LN_2 heat exchanger and then dropped back into the main cryostat after a LN_2 cooled Oxysorb^{TM} filtering. Forced re-circulation in liquid phase was instead designed to massively purify LAr to reach and maintain the highest purity level and permit a fast restoration of the argon purity in case of accidental pollution. LAr was extracted at a medium height on one side of the vessel, purified and injected back at the opposite longitudinal side 20 m apart close to the module bottom. The maximum re-circulation rate resulted to be about 1.5 m^3/h/unit.

The purity level of LAr was continuously monitored with an automatic tool to provide feed-back to the cryogenic plant operation and permit the correct estimation of the ionization charge and energy deposition in the recorded events. The electron lifetime τ has been measured on an event-by-event basis studying the attenuation $\lambda = 1/\tau$ of the charge signal of sufficiently long and clean cosmic muon tracks traversing the detector volume as a function of the electron drift distance. The charge signal was measured in the Collection plane after the removal of the noisy channels.

With the liquid re-circulation turned on, the LAr purity steadily increased in similar way in both modules, the electron lifetime exceeding 7 ms for the most part of the ICARUS data taking. It corresponds to a 12% maximum charge attenuation for the 1.5 m maximum drift distance (Figure 3).

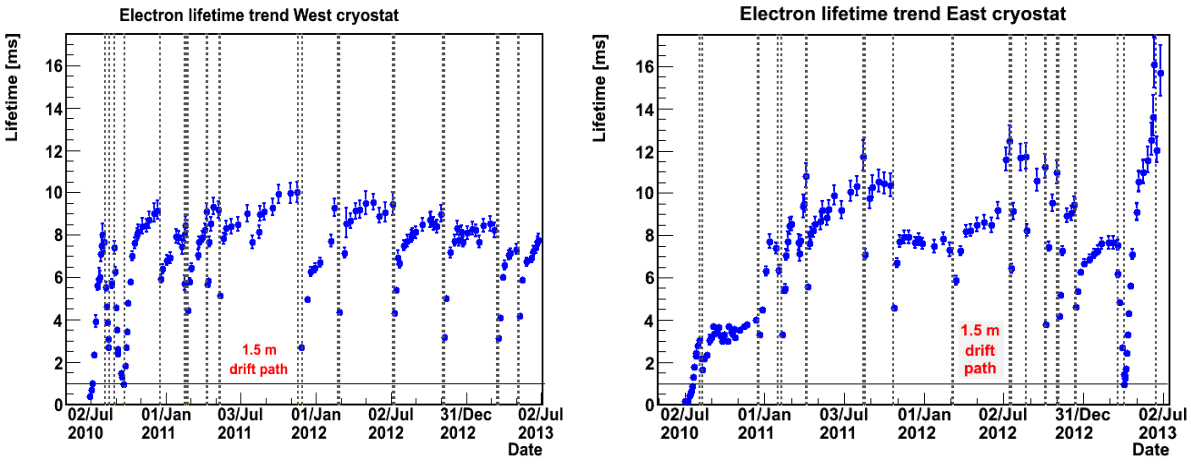

Figure 3. Electron lifetime τ of the West (left) and of the East module (right) for the whole ICARUS data taking. The dashed vertical lines represent the stops and restart of the LAr recirculation (during these periods gaseous Ar recirculation system continued to operate).

Unfortunately, along the three-years run several LAr re-circulation pump failures were experienced, promptly solved (in two to five days) by the pump redundancy, adequate spare equipment and accurate intervention procedure.

Purity was rapidly restored as soon as the LAr re-circulation was reactivated. The free electron lifetime was always maintained above the 3 ms threshold limit (0.1 ppb impurity concentration) all over the run without affecting the T600 detector operation and performance.

In addition, the introduction of the new Barber Nichols BNCP-32C-000 pump in April 2013 allowed to reach an electron lifetime of $16.1^{+1.3}_{-1.1}$ ms (6% maximum signal attenuation at longest drift distance) still rising at the end of the detector data taking, as shown in Figure 3 right. The obtained > 15 ms free electron lifetime corresponds to a mean attenuation length of about 25 meters and represents a milestone for the next generation of LAr TPC detectors. The LAr purity uniformity over the large ICARUS detector volume was checked by the λ stability with respect to its average value along the detector length with about 1000 almost vertical cosmic muons (Figure 4).

As a conclusion, the re-liquefaction system demonstrated to efficiently cover the maximum T600 cold power request with flexibility and margin guaranteeing a nitrogen closed loop operation. All the safety, control and supervision systems demonstrated to be extremely reliable and efficient. It has to be noted that the T600 detector continuous operation was never affected by intrinsic cryogenic plant faults. The liquid argon temperature uniformity was within 0.25 K and the argon pressure/temperature stability was extremely high. An upgrade of the LAr re-circulation system involving a more reliable pump was implemented and successfully tested during the T600 run at LNGS, resulting a useful development for future projects.

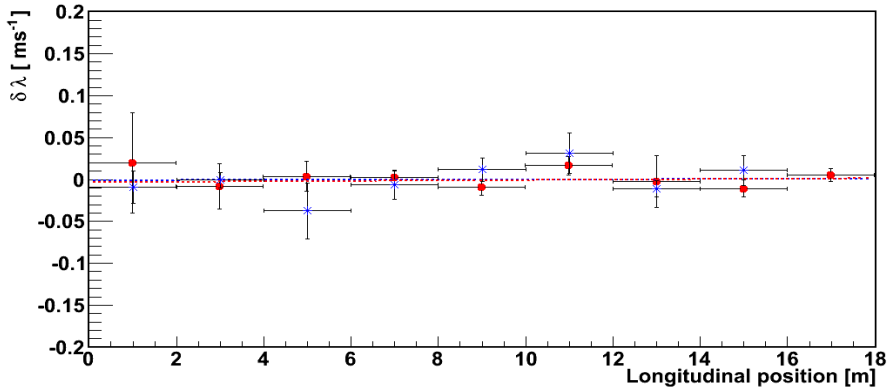

Figure 4. The measured variation of λ with respect to its average value $\delta\lambda = \lambda - \langle\lambda\rangle$ along the longitudinal direction for the left chamber (red circle) and the right one (blue star). The corresponding linear fits (dashed lines) are amply compatible with a uniform LAr purity across the length of the whole detector: slope for the left chamber $(8.8 \pm 90) \cdot 10^{-5}$ $ms^{-1}m^{-1}$, slope for the right chamber (2.7 ± 11) 10^{-4} $ms^{-1}m^{-1}$.

5 The ICARUS Trigger System

ICARUS-T600 LAr-TPC relies on its self-triggering capability using both scintillation light and charge signals produced by ionizing particles in LAr to detect CNGS neutrino interactions clustered in 10÷35 GeV energy range as well as cosmic-ray induced events, spanning a wide interval in energy deposition of events with topologies significantly different from each other [P19].

The scintillation light trigger system was built from the PMT light signals, integrated to exploit also the slow component of scintillation light (1.6 μs decay time). The sum of the PMT signals from each TPC chamber, properly discriminated, was sent to the detector Trigger Manager (see Figure 5).

A second independent source of trigger based on the charge recognition on adjacent wires in the chambers, was gradually implemented in the read-out boards, through Super Daedalus (SD) add-on, to increase the detection efficiency at low energy events down to few MeV. This SD system exploited a Double Rebinning sliding window (DR-slw) algorithm detecting the ionizing tracks through a digital filter of the wire signals above a suitable threshold and combining adjacent wire signals within a majority logic [2].

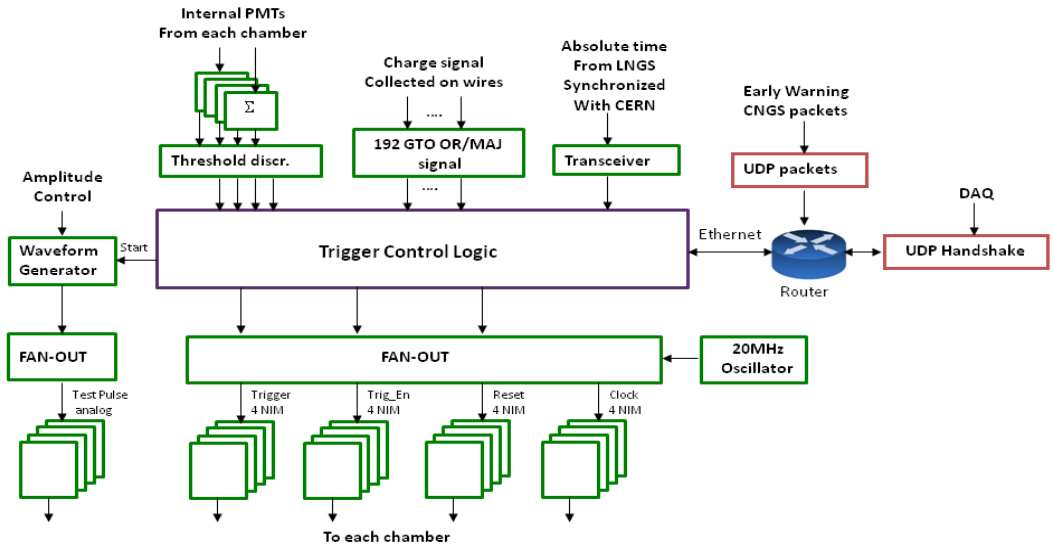

Figure 5 Block diagram of the ICARUS T600 Trigger Manager.

The T600 synchronization with the CNGS neutrino beam was achieved by means of a common GPS time base, shared at the CERN and LNGS sites. A 60 ms on-line CNGS-gate in coincidence with the arrival of neutrino bunch was generated at LNGS exploiting the "early warning" signal of the CERN SPS proton spill extraction sent from CERN, delayed for the 2.44 ms CERN to Gran Sasso neutrino time-of-flight.

The main ICARUS T600 trigger for detecting CNGS beam related events required the coincidence of the PMT sum signal in at least one of the four TPC chambers within the CNGS gate. As a result, a few mHz trigger rate was almost steadily obtained during the run. The efficiency of the PMT CNGS trigger has been estimated starting from the corresponding PMT sum signal efficiencies for each TPC measured with cosmic muons: the requirement of the PMT sum signal in at least one TPC per module guaranteed an almost full efficiency for an energy deposition E_{Dep} > 300 MeV in both cryostats (see Figure 6 left).

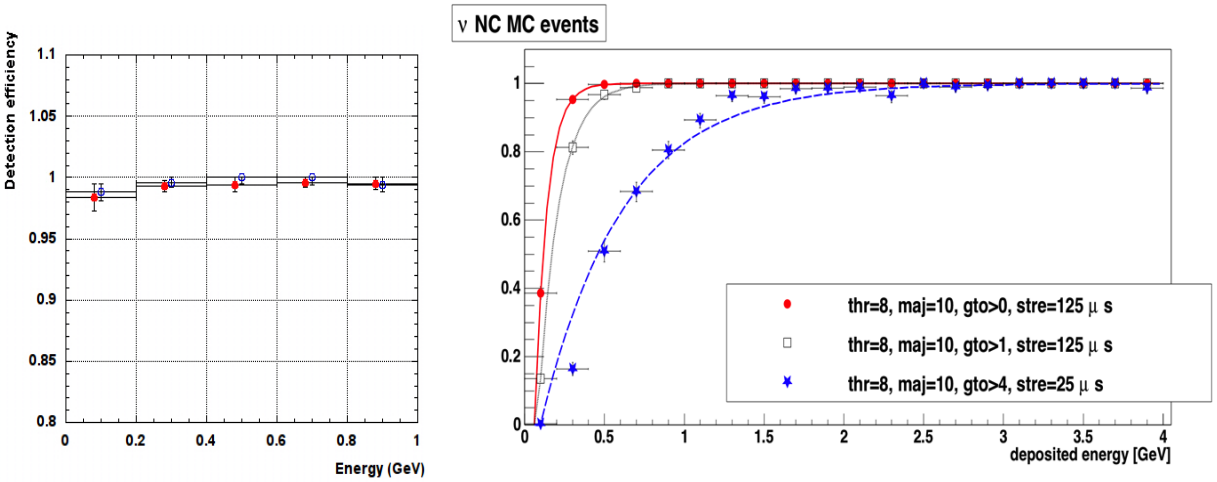

Figure 6 Left: efficiency of the CNGS PMT trigger in the West (red) and East (blue) module, as a function of deposited energy for cosmic muons. Right: SD CNGS trigger efficiency for ν NC Monte Carlo events as a function of the deposited energy, for three SD parameter configurations.

The efficiency of the SD charge trigger for the CNGS events has been evaluated on 10^4 νeCC, νNC and νμCC MC samples. For proper SD parameters choices, 99% and 91% trigger efficiencies were obtained, respectively for CC and for the most demanding NC interactions (Figure 6 right).

The SD trigger allowed also to directly qualify the PMT trigger on the basis of a "minimum bias" request, i.e. the presence of a ~5 cm long track in the TPCs. A ~2.5 10^{19} pot event statistic was collected with the SD trigger with a ~150 rejection factor of fake events, proving the almost full PMT trigger efficiency for both ν interactions in the detector active volume and crossing muons.

Cosmic-ray induced events have been triggered with an efficiency exceeding 90% requiring the coincidence of the PMT sum signals in two adjacent TPC chambers or in the presence of a single SD minimum bias signal out of the CNGS spill gate. The SD trigger allowed to significantly increase the detection efficiency below 500 MeV energy deposition.

The successful operation of the ICARUS T600 trigger system covering a wide range of event energies allowed the acquisition of CNGS and cosmic events with high reliability, efficiency and live-time, representing a robust baseline for future developments in multi-kton LAr-TPC neutrino detectors.

6 Tools for event reconstruction in LAr TPC

The quality of the information recorded by ICARUS, including bubble chamber like reconstruction of the event topology and the calorimetric measurement of both global deposited energy and local ionization density is perfectly suitable for detailed visual analysis of the event. However, the analysis of the large amount of data collected during CNGS and cosmic runs required the use of automatic tools, to assist and complement the visual scanning. Several independent algorithms were developed and tested for each step of data analysis from the identification of single wire signals (hit) to the reconstruction of tracks. For instance, the 2D segmentation, developed on MC to identify separate "clusters" in single views, has been widely used in analysis, including the reconstruction of long tracks and of stopping muons for the Multiple Scattering. Special filters for the rejection of incoming cosmic rays and the localization of the interaction vertex were used for atmospheric neutrino search. Moreover, the large statistics and different topologies of collected events allowed to tune and optimize the event reconstruction from the real data themselves, like the dependence of the reconstruction quality on the track inclination with respect to the wire planes.

An innovative approach to the 3D track reconstruction was developed and tested [P18] to avoid the artifacts and wrong associations in the match of individual hits on different 2D projections on the basis of their drift time. The new algorithm builds directly 3D objects by simultaneous optimization and matching of all the identified hits. This approach was applied in the reconstruction of tracks, cascade-like objects, interaction vertex regions as well as in the global event analysis, with excellent performance and permitting effective particle identification by dE/dx.

As an example a CNGS event with a decaying kaon is shown in Figure 7. Hits belonging to the decay chain (kaon, muon, and electron/positron) were used in the reconstruction. The event is correctly reconstructed in 3D resolving the narrow angle between kaon and muon and the overlap of electron/positron with the kaon track in Induction2 view. The nature of particle produced in the decay is correctly identified by the adopted Pid procedure.

A new method to analyze the most demanding part of event - the interaction vertex area - based on the image recognition technique using a neural network analysis has been developed. This innovative method can be used for automatic determination of the interaction point, estimation of the number of tracks exiting the interaction vertex as well as primary particle identification.

The data analysis tool and the track reconstruction solutions developed for the ICARUS experiment at LNGS will be crucial in the context of the next SBN short baseline neutrino experiment at Fermilab and of future long baseline experiments with LAr-TPC detectors.

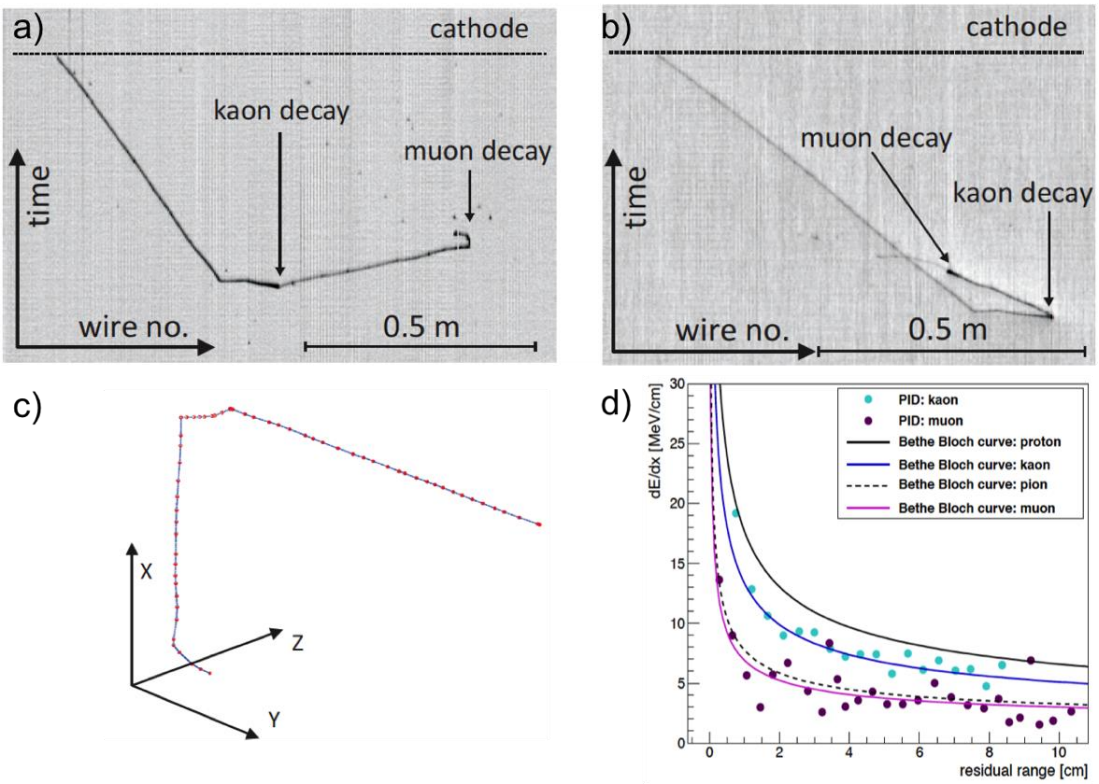

Figure 7: Kaon decay identified in the CNGS data and reconstructed using the automatic 3D reconstruction algorithm in Collection a) and Induction 2 b) projections. The 3D reconstruction and the PID are shown in c) and d) respectively.

7 Muon momentum measurement

The measurement of muon momentum via multiple Coulomb scattering (MCS) is fundamental for the reconstruction of ν_μ charged current interaction in ICARUS, since most muons escape the detector preventing a calorimetric measurement.

A dedicated algorithm has been developed and validated on a sample of ~1000 muons produced in CNGS neutrino interaction in the upstream rock, and stopping/decaying within the TPC fiducial volume; this sample provided a good benchmark, allowing an event-by-event comparison of the momentum p_{MCS} obtained from MCS with the corresponding calorimetric measurement p_{CAL}. Moreover, the momentum of these muons (~1 to ~5 GeV/c) largely corresponds to the momentum range of in future short- and long-baseline neutrino experiments. The developed algorithm is based on a statistical analysis of deflections between consecutive segments (L_{seg} ~19 cm) of muon tracks in Collection view, exploiting both the position of the segment barycenter and the segment direction obtained from a linear fit. The p_{MCS} value is estimated by comparing the observed deflection angles with the expectations from MCS as a function of muon momentum, accounting also for the measurement errors which could introduce apparent track deflections.

The results of the algorithm validation on stopping muons, also described in the last Report to SPSC in June 2016, are summarized in Figure 8: p_{MCS} and p_{CAL} are in good agreement, confirming the viability of MCS momentum measurement in a LAr-TPC. For tracks longer than 5 meters, using the first 4 meters for momentum measurement, the average resolution results $\Delta p/p$~15% in the stopping muon range. As expected, the resolution improves at smaller momentum and for longer tracks, as illustrated in Figure 9.

A slightly decreasing trend of p_{MCS} versus p_{CAL} has been observed at highest momenta, due to the deviations from planarity of the cathode (up to ±25 mm) as measured with laser-meters in East module during the T600 refurbishing at CERN, and independently by analyzing cosmic muons crossing the cathode at LNGS. This mechanical distortion

introduced slight drift field dis-uniformities which affect the reconstructed drift coordinate mimicking track deflections. The consequent underestimate of p_{MCS} w.r.t. p_{CAL}, while negligible at low energy, can reach ~15% at higher momentum (over ~3 GeV/c), as shown in Figure 10.

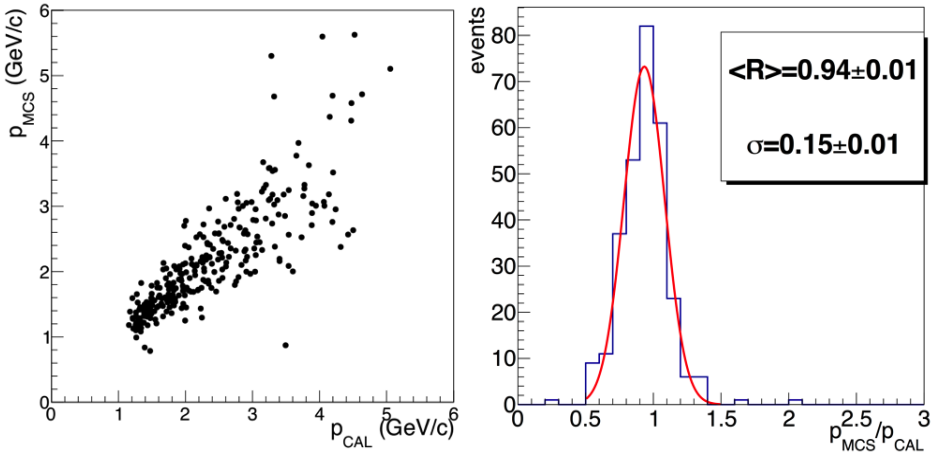

Figure 8. Scatter-plot of p_{MCS} vs. p_{CAL} (left) and distribution of the p_{MCS}/p_{CAL} ratio (right) for the full stopping μ sample. Only the first 4 m of the μ track are used, requiring the μ length >5 meters (to simulate escaping muons).

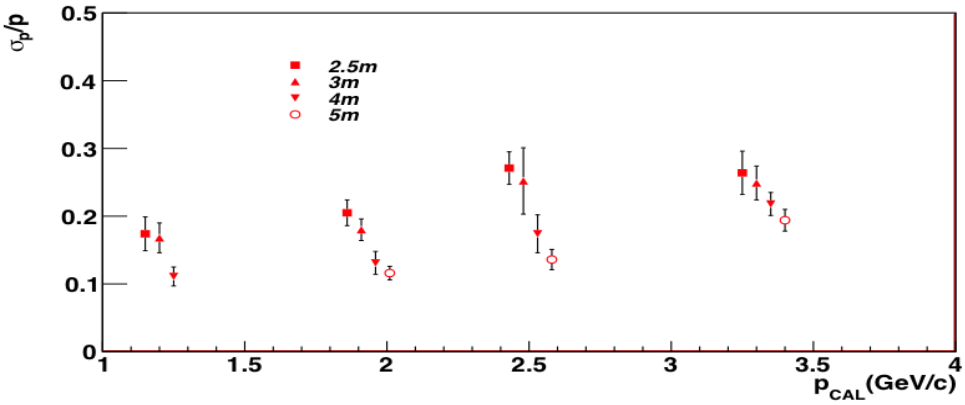

Figure 9. The p_{MCS} resolution as a function of p_{CAL} for four different used track lengths ranging from 2.5 to 5 m.

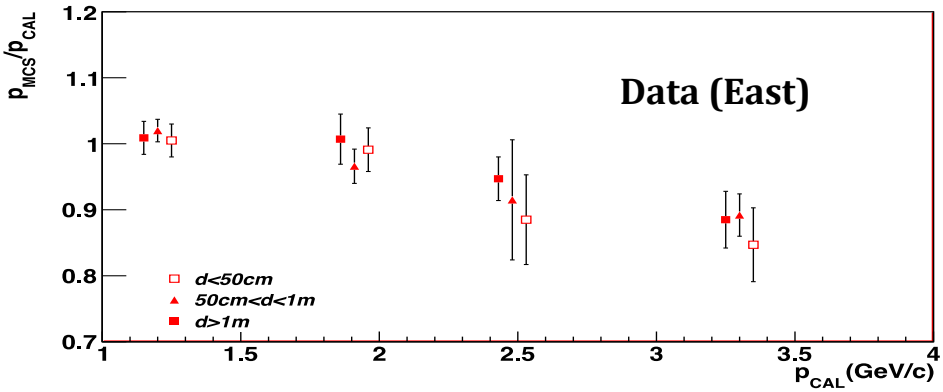

Figure 10. Dependency of p_{MCS}/p_{CAL} ratio on p_{CAL} (using 4 m of muon track length) for muons in the East module only; data have been grouped depending on the distance from the cathode. The average momenta p_{CAL} in each bin are shifted by ±50 MeV to enhance visibility.

To quantitatively estimate the effect of cathode non-planarity on muon momentum, a full 3D simulation has been performed with the COMSOL Multiphysics® software. The electric field configuration has been calculated with a 2.5 cm mesh, starting from the planarity map measured with the laser-meter. The resulting distortions in the reconstructed drift coordinate extend up to few centimeters, as described in detail in the Report to SPSC in 2016.

The rough geometrical resolution of the COMSOL simulation, however, does not allow to fully describe the fine structure of the cathode and of the field cage electrodes, therefore preventing a point-by-point correction of the muon track distortion. An average estimation of the cathode distortion effect on MCS measurement has been computed by MonteCarlo simulations, obtaining the ratio $R=(p_{MCS}/p_{CAL})_{MC}$ as a function of muon momentum and distance from the cathode. For each real stopping muon, the average correction $1/R$ resulted in a strong reduction of the underestimation down to ~5%, as shown in Figure 11.

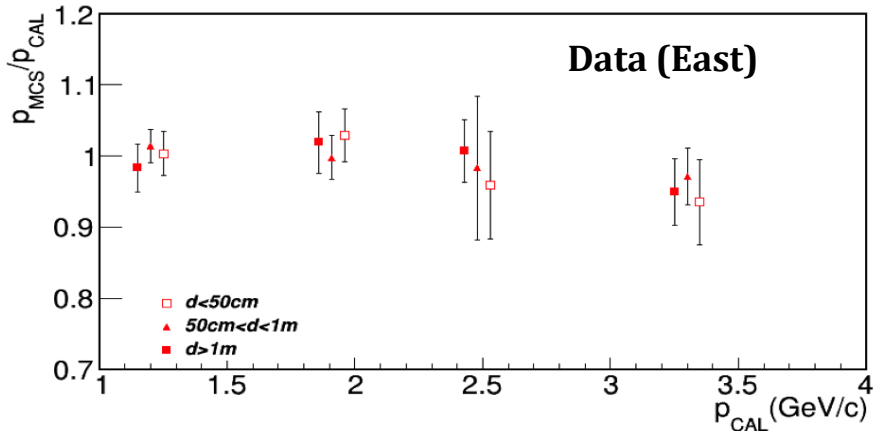

Figure 11. Dependency of p_{MCS}/p_{CAL} ratio on p_{CAL} (using a muon length of 4 m) for CNGS muons stopping in the East module (3 bins of muon distance from the cathode) after the average correction for the cathode deviations from planarity as determined from the corresponding MC calculation. The average momenta p_{CAL} in each bin (on the horizontal axis) are shifted by ±50 MeV to enhance visibility.

The measurement of muon momentum by MCS will also be crucial for the study of ν_μCC interaction in the future SBN experiment at FNAL; the present algorithm will be directly applied to this case, after an optimization of the segment length, to account for the lower muon momentum (< 1 GeV/c) and shorter muon track lengths.

The T600 refurbishing at CERN, which ended in March 2017 before the imminent detector transportation to FNAL, addressed the issue of the cathode distortion, reducing its deviations from planarity to a few millimeters, resulting in a strong reduction of its impact on MCS momentum measurement. Moreover, the improved TPC read-out electronics with the full synchronization of the ADC sampling times for all wires will allow to improve the muon track reconstruction, resulting in a ~20% improvement in momentum resolution. A more detailed description of the measurement algorithm and its validation on the stopping muon sample can be found in the paper [P15].

8 Search for anomalous ν_e appearance in the CNGS beam

The CERN CNGS neutrino facility delivered an almost pure ν_μ beam clustered in 10÷30 GeV energy range, with a ~1 % intrinsic electron component [15]. The events collected during the 2010-2012 run with the dedicated CNGS trigger (see section 5) were analyzed to select the neutrino interactions after the initial automatic data preprocessing which removed empty events and events affected by mismatch with the trigger source information. A total statistic of 2650 neutrino interactions, corresponding to an analyzed sample of $7.93\cdot10^{19}$ pot, was identified in the "scanning fiducial volume" (1.5 cm from the TPC walls, 5 cm from the upstream wall and 15 cm from the downstream wall), in rough agreement with the corresponding MC expectations. The total visible energy of neutrino events was

determined from the charge collected by the TPC wires and corrected for the response of electronic read out, the electron lifetime attenuation and recombination effects. The neutrino interaction vertex and 2D projections of tracks and showers were visually identified.

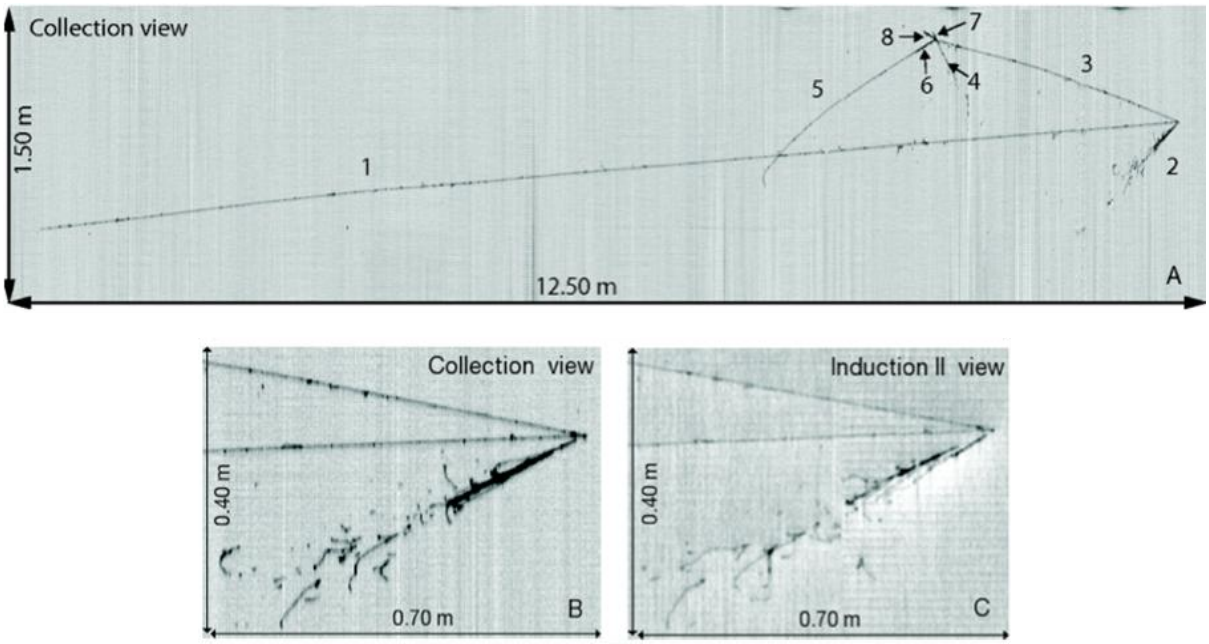

Figure 12. An example of ν_μCC interaction from the CNGS beam (Collection view) with a ~13 m long muon track [A]; a close-up view of the primary vertex for the Collection [B] and Induction-2 [C] projections allows to solve completely the event topology.

The ν_μ and anti-ν_μ charged current (CC) events were further selected, with a ~70% efficiency and a rejection factor 60 for NC events, requiring the μ candidate track to be longer than 2.5 m (see an example in **Figure 12**). Globally 1285 ν_μ and anti- ν_μ CC events have been selected in a 6.7 x 10^{19} pot event statistics corresponding to the 2011 and 2012 runs. All these events have been visually measured and reconstructed in detail separating muon tracks from accompanying hadronic jet. Undetected neutrals and particles escaping the detector were accounted for by correcting on average the deposited energy of hadronic jet as a function of the distance from the external walls of the detector. Corrections were computed by a dedicated MC study in which only the hadrons produced by CNGS neutrino interactions were simulated (primary muons were not propagated through the detector). The corrected hadronic energy appears to be in reasonable agreement with the corresponding hadron energy (E_{had}) in the FLUKA simulation [12][13], see Figure 13. The corresponding measured muon length is ~7.5 m on average and appears to be reproduced by the MC, as shown in Figure 14.

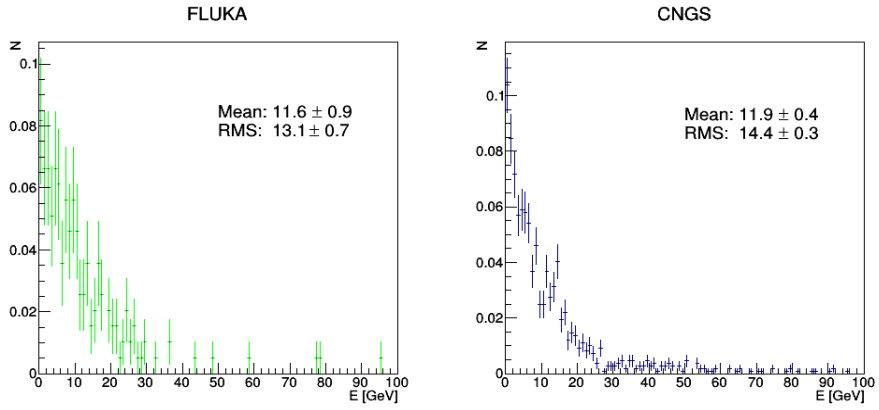

Figure 13. The corrected Hadron energy for MC (left) and Data (right).

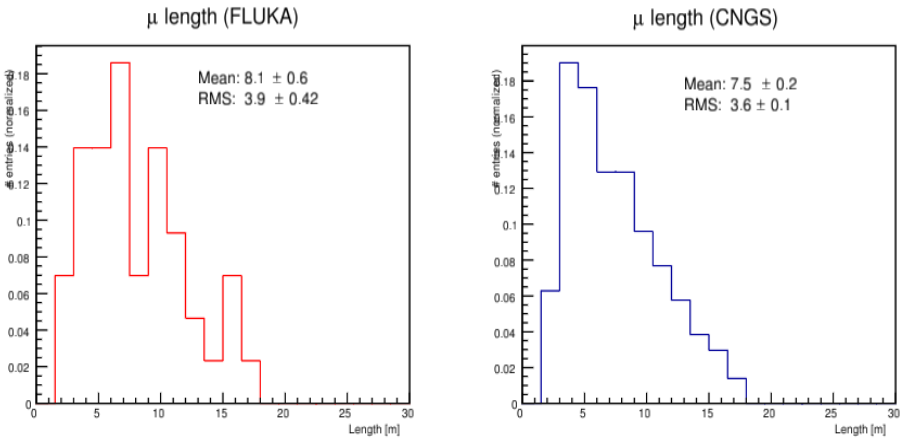

Figure 14. Reconstructed muon track length distribution (in meters), normalized to unity, from ν_μ and anti-ν_μ CC interactions: Monte Carlo, FLUKA (left) and data (right).

ICARUS performed a sensitive search for a $\nu_\mu \rightarrow \nu_e$ event excess related to $L/E_\nu \approx 1$ m/MeV anomaly first reported by the LSND experiment [6] at the LANSCE Los Alamos accelerator and then by the MiniBooNE experiment [7] at the FNAL-Booster beam. Additional ν_e or anti-ν_e disappearance anomalies have been observed at similar Δm^2_{new} values in nearby nuclear reactors [10][11] and in solar neutrino experiments, using Mega-Curie k-capture radioactive sources [8][9]. These anomalies may imply the existence of new sterile neutrino flavors with additional mass-squared differences in a wide interval $\Delta m^2_{new} \approx 0.01$ to 1.0 eV^2 in excess with respect to the prediction of the three-neutrino mixing model.

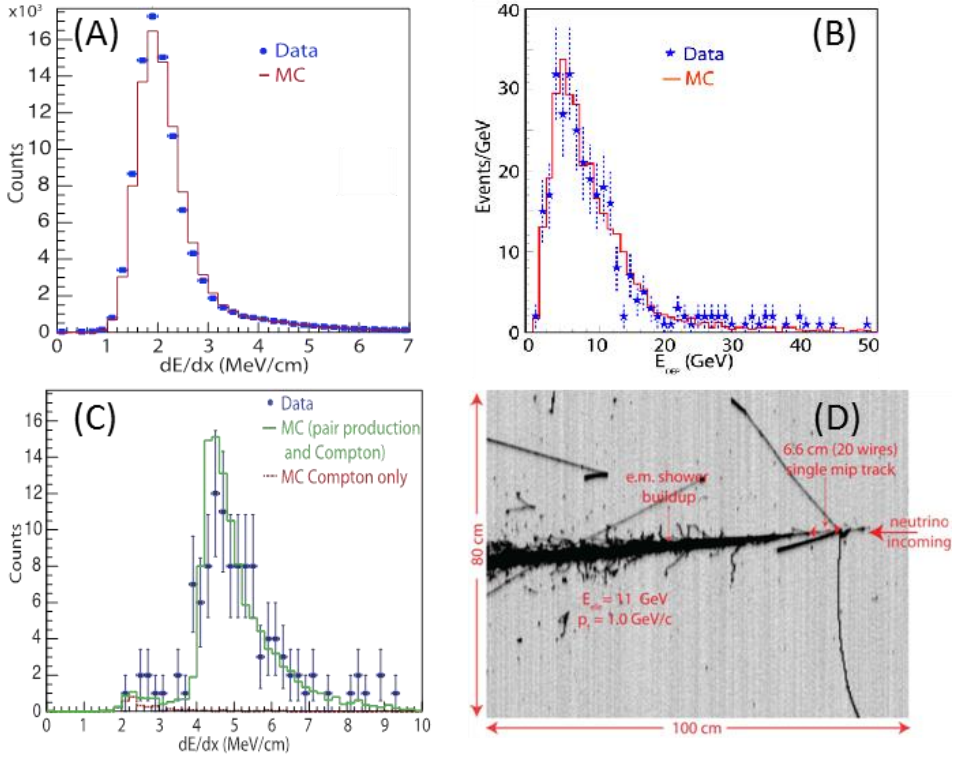

Figure 15. Comparison of data with simulations: (A) Energy deposition density distribution for muons in CNGS CC interactions; Experimental raw energy distribution E_{dep} for νμ and anti νμ CC interaction in the ICARUS T600 detector; (C) Average ionization in the first 8 wire hits for sub-GeV photons in the T600 data (in MC case, the Compton contribution is shown also separately, dotted red line). (D): Typical M.C. generated $\nu_\mu \rightarrow \nu_e$ event from the ICARUS full simulation program [12][14] with E_e =11 GeV and p_T = 1.0 GeV/c. The close similarity of the MC simulation with actual ICARUS events (see Figure 17) is apparent.

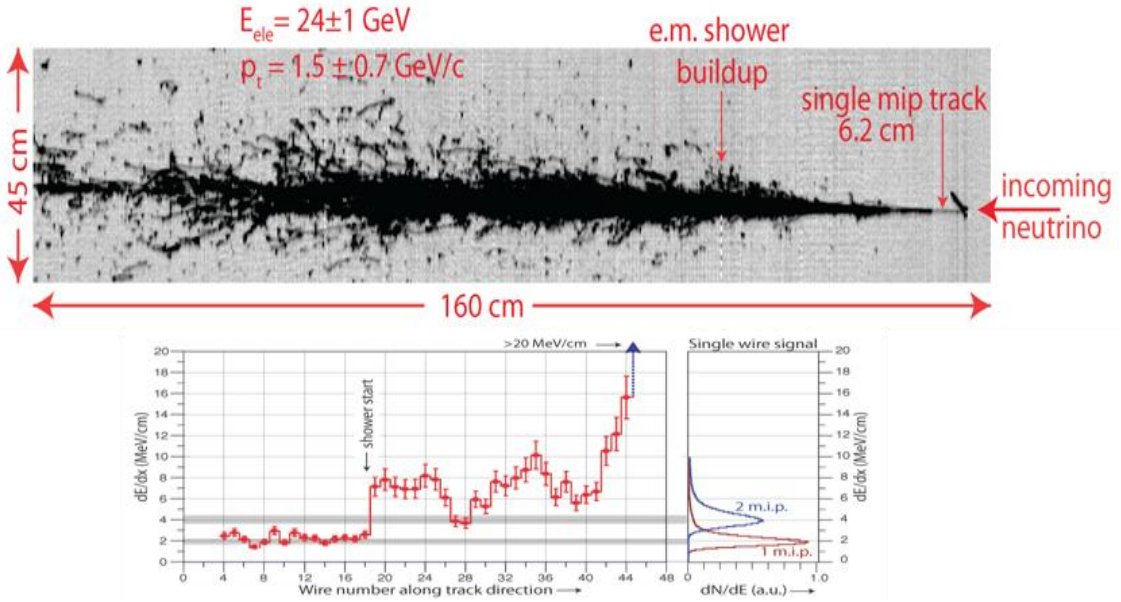

Figure 16. A CNGS event with clear electron signature (left): the primary electron has energy 24.0 ± 1.0 GeV and transverse momentum of 1.5 ± 0.7 GeV/c. The evolution of the actual dE/dx from a single track to an e.m. shower for the electron shower is shown along the individual wires (right).

The CNGS beam baseline (L/E ≈ 36.5 m/MeV) was very different from the LSND one: a LSND-like short distance oscillation signal would be averaged to $\sin^2(1.27\,\Delta m^2_{new}\,L/E_\nu) \approx ½$ and $\langle P_{\nu\mu\to\nu e}\rangle = ½\,\sin^2(2\theta_{new})$.

In order to reproduce the signals from the actual events, a sophisticated simulation package based on FLUKA [12][13] has been developed, including the neutrino event generator reported in [14][P9]. The simulation accounted also for the experimentally observed recombination effects [P3] as well as readout channel response (wire signal induction and electronics response) and noise parameters measured in the data. Such a procedure resulted in a remarkably close similarity between real and simulated neutrino events (see Figure 17).

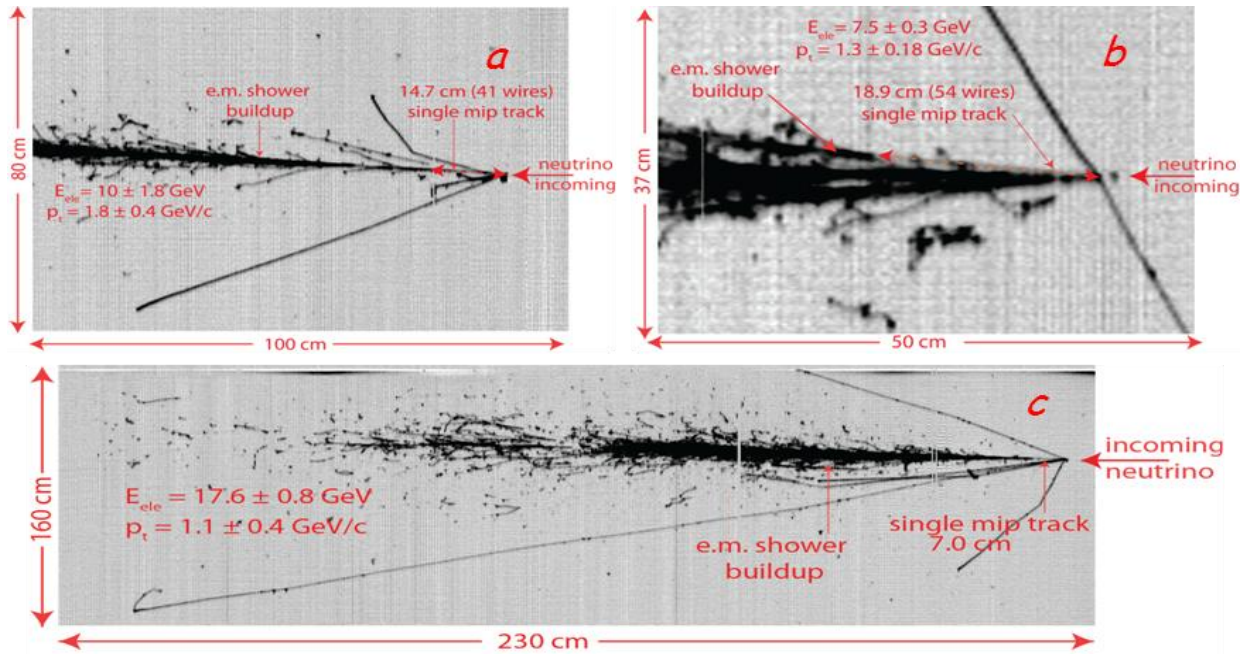

Figure 17. Some additional examples of ν_e events identified in the CNGS beam.

A reduction of 50% of the intrinsic ν_e background with only a 15 % reduction for the expected signal has been obtained by considering only the neutrino events with energy $E < 30$ GeV. The visual "electron neutrino signature" was requiring in addition: 1) a primary charged track starting from the vertex fully consistent with a single m.i.p. relativistic particle and subsequently building up into a shower; 2) the electron candidate track with a visible spatial separation from the other ionizing tracks within 150 mrad near the vertex. The corresponding selection efficiency has been evaluated to be 0.74 ± 0.05 for the expected signal and 0.65 ± 0.06 for the expected intrinsic ν_e contamination.

Globally in the analyzed statistics 7 electron neutrino events have been identified (see Figure 16 and Figure 17) to be compared to 8.4 ± 1.1 expected ν_e interactions due to conventional sources. As a result the corresponding limits on the oscillation probability due to the LSND anomaly are $\langle P(\nu\mu \rightarrow \nu e)\rangle \leq 3.92 \times 10^{-3}$ and $\langle P(\nu\mu \rightarrow \nu e)\rangle \leq 7.83 \times 10^{-3}$, at 90% and 99% CL respectively, in a two flavor oscillation framework. A detailed comparison between the various experimental results is shown in Figure 18.

While for $\Delta m^2 >> 1\ eV^2$ there is a general disagreement between the allowable regions from the published experiments, for $\Delta m^2 \leq 1\ eV^2$ the ICARUS results allowed to define a much smaller, narrower region in which there was 90 % CL agreement between (1) the present ICARUS limit, (2) the limits of KARMEN and (3) the positive signals of LSND and MiniBooNE collaborations. Therefore, a definitive experiment would be required to clarify at >5 σ level the nature of all reported anomalies.

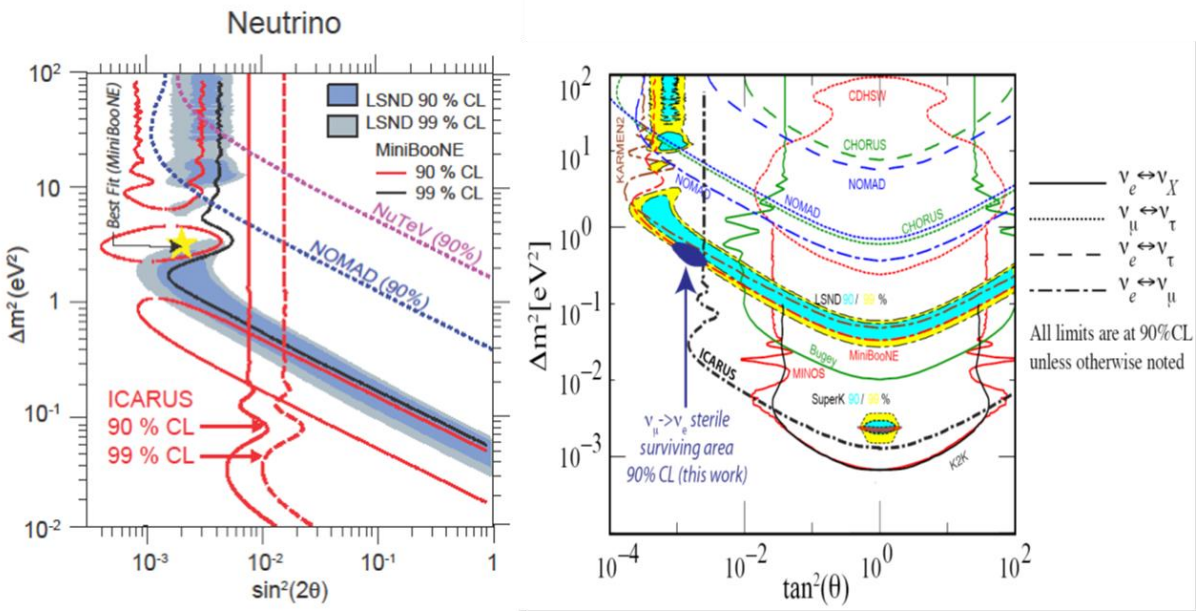

Figure 18. Left: ($\sin^2 2\theta_{new}$, Δm^2_{new}) plot for the different experiments sensitive to the $\nu_\mu \rightarrow \nu_e$ anomaly and the 90 % and 99 % CL ICARUS exclusion curves (left). Rigth: the blue area indicates the region where there was agreement between all experimental results at accelerators [P17].

9 Addressing the Superluminal neutrino problem

ICARUS addressed also the superluminal neutrino anomaly hinting at $\delta = (v_\nu^2 - c^2)/c^2 = 5 \times 10^{-5}$ deviation of the neutrino velocity from the light velocity [3]. As argued by A.G. Cohen and S.L. Glashow super-luminal muon neutrinos should lose their energy by producing photons and e^+e^- pairs, through Z^0 mediated processes analogous to Cerenkov radiation, resulting in a full ν event suppression above 30 GeV and ~10^7 isolated e^+e^-

pairs/10^{19} p.o.t./kt (E_{dep} > 200 MeV within 150 mrad from CNGS beam axis)[4]. However, ICARUS did not observe these effects in the recorded data (see Figure 19) setting a 90 % CL limit for $\delta < 2.5 \times 10^{-8}$ [P12].

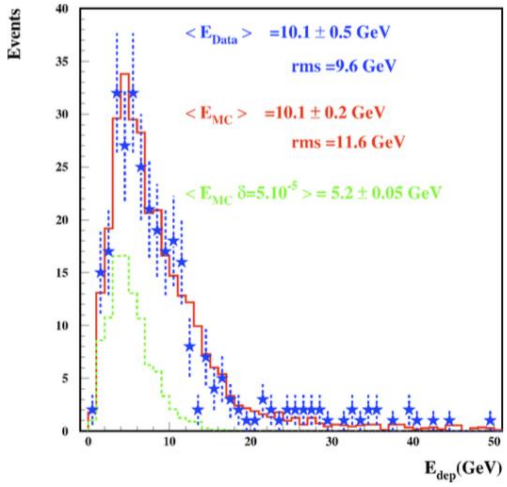

Figure 19. Experimental raw energy E_{dep} distribution for νμ and anti-νμ CC interactions in ICARUS (blue) compared with MC expectations for an unperturbed spectrum (red), and for $\delta = 5\times10^{-5}$ (green). 1.53×10^{19} p.o.t. were used for the analysis.

At the end of the 2011 run, the CNGS neutrino beam was briefly operated in lower intensity mode with a bunched proton beam (~3 ns wide) allowing for a first neutrino time-of-flight measurement on an event-by-event basis. ICARUS detector collected 7 beam-associated events measuring a difference $\delta t = tof_c - tof_\nu = +0.3 \pm 4.9_{stat} \pm 9.0_{syst}$ ns [P12] (see Figure 20 Left). In 2012 two additional weeks of bunched beam were provided (64 bunches, 4ns FWHM each), a more accurate and redundant synchronization between CERN and LNGS was put into operation and the baseline was re-measured with high precision geodesy. ICARUS took part to this measurement campaign with an additional PMT-DAQ system, digitizing at 1 GHz sampling rate both higher granularity PMT-sum signals and various control and synchronization signals providing absolute references from the global CERN-LNGS timing systems.

During this second bunched beam run, ICARUS collected 25 beam-associated events, measuring event by event the neutrino tof_ν exploiting the full redundancy of the specially designed timing synchronization set-up (Figure 20 Right). The resulting average value $\delta t = +0.10 \pm 0.67_{stat} \pm 2.39_{syst}$ ns is fully compatible with the neutrino propagation at the speed of light, excluding neutrino velocities exceeding the speed of light by more than 1.35×10^{-6} c at 90 % C.L. [P14].

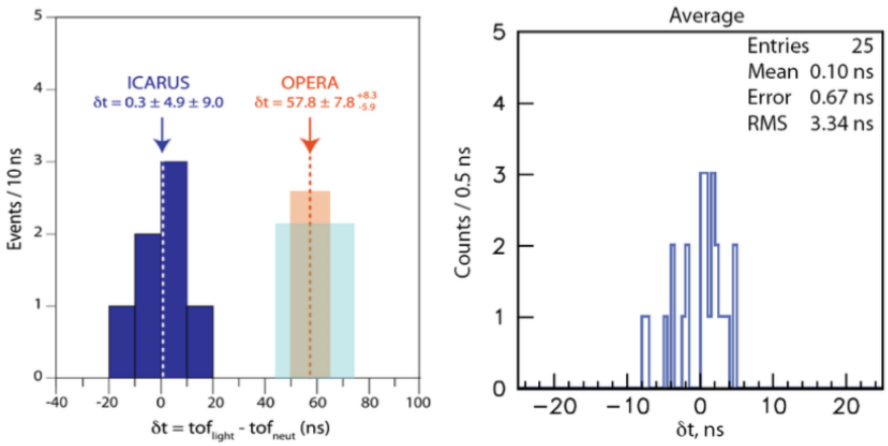

Figure 20. [Left]: Bunched beam campaign 2011: event distribution in ICARUS for δt = tofc - tofv. The first OPERA claim that motivated the neutrino velocity measurement with ICARUS is also shown. [Right]: Bunched beam campaign 2012: event distribution in ICARUS for $\delta t = tof_c - tof_\nu$., according to the averaging procedure of all synchronization paths.

Besides the physical result, this study demonstrated the capability of LAr-TPC to measure with ns resolution the absolute time of individual events, combining the detection of prompt component of scintillation light in LAr and the accurate event geometrical reconstruction. This feature will be even more relevant in the next shallow depth operation of ICARUS at FNAL, where it will be fully exploited to cope with the abundant rate of cosmics crossing the detector and randomly overlapped to each triggered event.

10 Search for the atmospheric neutrino interactions

ICARUS collected cosmic ray data with a total exposure of 0.73 kt year. In particular, the events recorded during the 2012-2013 run (0.48 kt year), characterized by the best trigger conditions, have been analyzed aiming at the identification and study of atmospheric neutrino interactions inside the detector. The identification and reconstruction of these events, in particular the ν_eCC, have in itself a strong interest as a significant test bench in view of the future SBN experiment at FNAL. In fact they cover the energy range for the neutrino events expected at the Booster Neutrino Beam. At FNAL the detector will operate at shallow depth requiring the selection, identification and reconstruction of ν_eCC among the dominating ν_μCC and among the cosmic-rays randomly overlapped to each triggered event.

The search for neutrino interactions in the detector exploits an automatic procedure rejecting incoming cosmic rays and pre-selecting candidate events to be then validated by careful visual scanning. Actually this automatic procedure is organized into two independent branches, the first based on the search of interaction vertices inside the detector and the selection of multi-prong candidates with ~30% efficiency for both ν_eCC and ν_μCC. The second branch is optimized for the ν_eCC search with a faster processing based on an efficient rejection of long straight tracks associated to incoming and passing cosmic muons with ~70% and 18% efficiency for ν_eCC and ν_μCC respectively. Globally the amount of data needing visual validation is reduced by about a factor 100. So far ~42% and ~65% of the 2012-2013 run have been processed in the first and second branch respectively and visually analyzed, identifying 7 electron neutrino events and 7 ν_μ CC interactions in total with E_{DEP} in 0.2 ÷ 10 GeV range (see Figure 21). The analysis of the remaining fraction of events is ongoing, in particular one additional quasi-elastic νeCC event of ~0.9 GeV deposited energy has been identified (Figure 22).

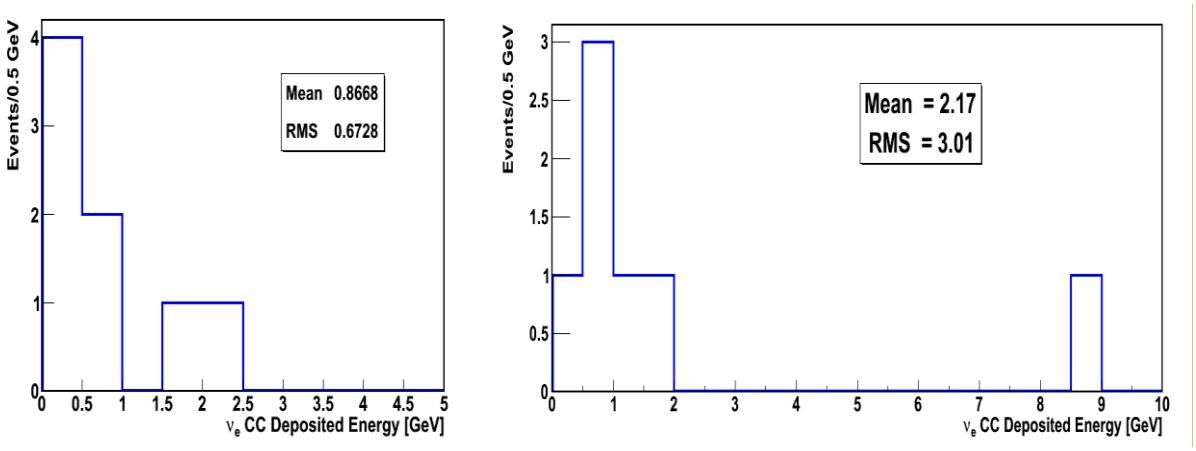

Figure 21. Distribution of total deposited energy of the atmospheric ν_e CC (left, including the additional event found so far in the ongoing analysis) and ν_μ CC (right) identified in the data.

A clear νμCC event with an up-going ~4 m long μ track and three charged particles, with a total deposited energy of 1.7 GeV is shown in Figure 23**.** The escaping muon momentum is estimated to be ~1.8 ± 0.3 GeV/c by measuring its multiple Coulomb scattering.

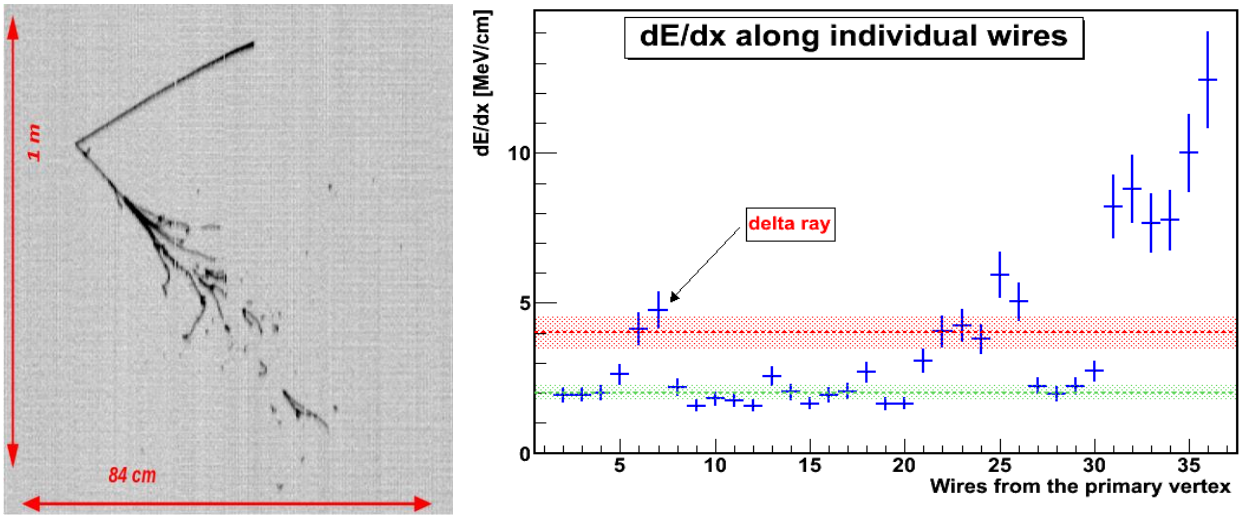

Figure 22. A quasi elastic electron-like atmospheric neutrino event candidate with deposited energy E_{dep} ~0.9 GeV (left, collection view). The hadronic track is identified as a proton by its dE/dx vs range. The plot on the left shows the evolution of the dE/dx from a single track to an e.m. shower for the primary electron: the green and red lines indicate the expected dE/dx for single m.i.p. and double m.i.p. respectively.

The adopted procedure to select atmospheric electron neutrino candidates permits, as by-product, to address nucleon decay search in selected channels involving kaons. Despite the limited ICARUS exposure, the superb quality of event visualization and reconstruction allows for a study on a single event basis with virtually zero background in $n \rightarrow e^{+}K^{-}$, a channel difficult to measure with large water Cherenkov detectors. A first study of MC events indicates an overall ≈80% selection and identification efficiency of the automatic pre-filter and the visual scanning procedure for this nucleon decay channel.

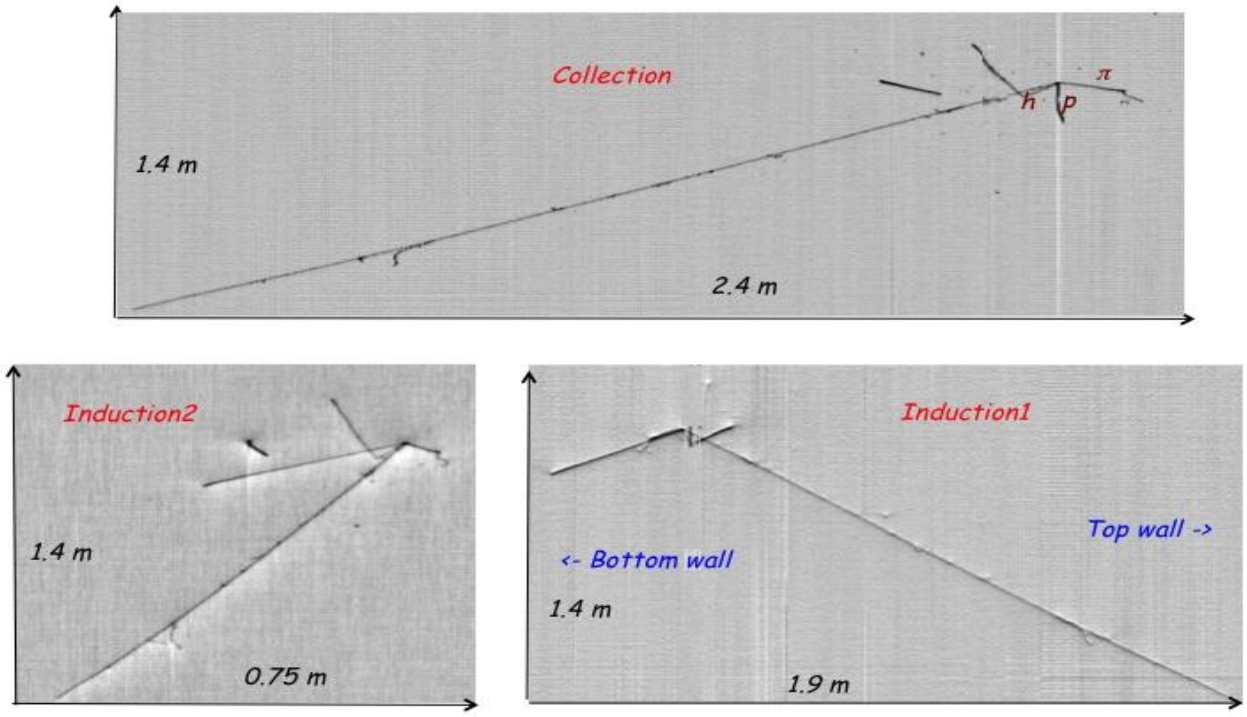

Figure 23. A clear upward-going atmospheric ν_{μ}CC candidate with E_{dep} = 1.7 GeV. The momentum of the 4 m escaping muon is measured to be 1.8 ± 0.3 GeV/c from multiple scattering (zenith angle ~52°). Three hadrons are produced in the neutrino interaction vertex, two of which are identified as a pion decaying in a muon followed by an electron (E_{dep} ~80 MeV) and a proton (E_{dep} ~ 250 MeV). The preliminarly reconstructed neutrino energy is ~2 GeV with a zenith angle ~78°.

11 Conclusions

The LAr-TPC detection technique has been taken to the full maturity with the realization of the ICARUS-T600, the biggest Liquid Argon detector ever realized, operated in the underground Gran Sasso Laboratory of INFN. It is a result of many years of R&D studies performed by the ICARUS Collaboration with the continuous support of INFN.

ICARUS-T600 detector completed in 2013 a successful continuous three year run at LNGS exposed to both CNGS neutrino beam and cosmic rays, obtaining remarkable physics and technical achievements which prove the validity of the single phase LAr-TPC technology for neutrino physics. The recorded events demonstrated the excellent detection performance of ICARUS as a tracking device and as a homogeneous calorimeter with remarkable particle identification capabilities exploiting the measurement of dE/dx vs. range.

ICARUS performed a sensitive search for a potential νe excess related to LSND-like anomalies in the high energy CNGS ν_μ beam defining a much smaller, narrower region in which all the experimental results can be accommodated at 90 % CL. The ability to reconstruct the neutrino interactions with complex event topologies in a broad energy range combined with the efficient identification of primary electrons allows to reject the backgrounds in the search for νμ→νe transitions at an unprecedented level.

In 2014 the ICARUS T600 detector has been moved to CERN for an extensive overhauling in view of the forthcoming SBN Program at FNAL [16] to perform sensitive searches for ν_e appearance and ν_μ disappearance in the 0.8 GeV Booster Neutrino Beam with three LAr-TPCs, SBND MicroBooNE and ICARUS at 110, 470 and 600 m from target respectively. The comparison of the ν spectra measured by ICARUS with those measured by SBND and MicroBooNE will allow to definitively settle the new ``sterile'' neutrino state covering the LSND anomaly parameter region, with 5 σ CL in three years data taking.

All the obtained results mark a milestone for the LAr-TPC technology with a large impact on the future neutrino and astro-particle physics projects, like the current FNAL SBN short-baseline neutrino program with three LAr-TPC detectors, and the considered long-baseline DUNE project with a multi-kt LAr-TPC detector.

List of selected ICARUS publications

[P1] F. Arneodo et al. (ICARUS Collaboration), "*Observation of long ionizing tracks with the ICARUS T600 first half-module*", Nuclear Instruments and Methods in Physics Research, Section A: Accelerators, Spectrometers, Detectors and Associated Equipment, 508 (3), pp. 287-294 (2003). DOI: 10.1016/S0168-9002(03)01508-0.

[P2] S. Amoruso et al. (ICARUS Collaboration), "*Analysis of the liquid argon purity in the ICARUS T600 TPC*", Nuclear Instruments and Methods in Physics Research, Section A: Accelerators, Spectrometers, Detectors and Associated Equipment, 516 (1), pp. 68-79 (2004). DOI: 10.1016/j.nima.2003.07.043.

[P3] S. Amoruso et al. (ICARUS Collaboration), "*Study of electron recombination in liquid Argon with the ICARUS TPC*", Nuclear Instruments and Methods in Physics Research, Section A: Accelerators, Spectrometers, Detectors and Associated Equipment, 523 (3), pp. 275-286 (2004). DOI: 10.1016/j.nima.2003.11.423.

[P4] S. Amoruso et al. (ICARUS Collaboration), "*Measurement of the μ decay spectrum with the ICARUS liquid Argon TPC*" European Physical Journal C, 33 (2), pp. 233-241 (2004). DOI: 10.1140/epjc/s2004-01597-7.

[P5] S. Amerio et al. (ICARUS Collaboration), "*Design, construction and tests of the ICARUS T600 detector*", Nuclear Instruments and Methods in Physics Research, Section A: Accelerators,

Spectrometers, Detectors and Associated Equipment, 527 (3), pp. 329-410 (2004). DOI: 10.1016/j.nima.2004.02.044.

[P6] A. Ankowski et al. (ICARUS Collaboration), "*Characterization of ETL 9357FLA photomultiplier tubes for cryogenic temperature applications*", Nuclear Instruments and Methods in Physics Research, Section A: Accelerators, Spectrometers, Detectors and Associated Equipment, 556 (1), pp. 146-157 (2006). DOI: 10.1016/j.nima.2005.10.108.

[P7] C. Vignoli et al. (ICARUS Collaboration), "*ICARUS: an innovative large LAr detector for neutrino physics*", Advances in Cryogenic Engineering 51(2006) p 1643.

[P8] A. Ankowski et al. (ICARUS Collaboration), "*Measurement of through-going particle momentum by means of multiple scattering with the ICARUS T600 TPC*", European Physical Journal C, 48 (2), pp. 667-676 (2006). DOI: 10.1140/epjc/s10052-006-0051-3.

[P9] F. Arneodo et al., (ICARUS and Milano Collaborations), "*Performance of a liquid argon time projection chamber exposed to the CERN West Area Neutrino Facility neutrino beam*" Phys. Rev. D 74, pp. 112001-112015 (2006). DOI: 10.1103/PhysRevD.74.112001.

[P10] A. Ankowski et al. (ICARUS Collaboration), "*Energy reconstruction of electromagnetic showers from π0 decays with the ICARUS T600 liquid argon TPC*", Acta Phys. Pol. B, 41 (1), pp. 103-125 (2010).

[P11] C. Rubbia et al. (ICARUS Collaboration), "*Underground operation of the ICARUS T600 LAr-TPC: First results*", Journal of Instrumentation, 6 (7), art. no. P07011 (2011). DOI: 10.1088/1748-0221/6/07/P07011.

[P12] M. Antonello et al. (ICARUS Collaboration), "*A search for the analogue to Cherenkov radiation by high energy neutrinos at superluminal speeds in ICARUS*", Physics Letters, Section B: Nuclear, Elementary Particle and High-Energy Physics, 711 (3-4), pp. 270-275 (2012). DOI: 10.1016/j.physletb.2012.04.014.

[P13] M. Antonello et al. (ICARUS Collaboration), "*Measurement of the neutrino velocity with the ICARUS detector at the CNGS beam*", Physics Letters, Section B: Nuclear, Elementary Particle and High-Energy Physics, 713 (1), pp. 17-22 (2012). DOI: 10.1016/j.physletb.2012.05.033.

[P14] M. Antonello et al. (ICARUS Collaboration), "*Precision measurement of the neutrino velocity with the ICARUS detector in the CNGS beam*", Journal of High Energy Physics, 2012 (11), art. no. 049 (2012). DOI: 10.1007/JHEP11(2012) 049.

[P15] M. Antonello et al. (ICARUS Collaboration), "*Muon momentum measurement in ICARUS-T600 LAr-TPC via multiple scattering in few-GeV range",* JINST 12 (2017) no.04, P04010.

[P16] M. Antonello et al. (ICARUS Collaboration), "*Experimental search for the "LSND anomaly" with the ICARUS detector in the CNGS neutrino beam*", European Physical Journal C, 73 (3), art. no. 2345, pp. 1-9 (2013). DOI: 10.1140/epjc/s10052-013-2345-6.

[P17] M. Antonello et al. (ICARUS Collaboration), "*Search for anomalies in the ve appearance from a νμ beam*", European Physical Journal C, 73 (10), art. no. 2599, pp. 1-6 (2013). DOI: 10.1140/epjc/s10052-013-2599-z.

[P18] M. Antonello et al. (ICARUS Collaboration), "*Precise 3D track reconstruction algorithm for the ICARUS T600 liquid argon time projection chamber detector*", Advances in High Energy Physics, 2013, art. no. 260820 (2013). DOI: 10.1155/2013/260820.

[P19] M. Antonello et al. (ICARUS Collaboration), "*The trigger system of the ICARUS experiment for the CNGS beam*", Journal of Instrumentation, 9 (8), art. no. P08003 (2014). DOI: 10.1088/1748-0221/9/08/P08003.

[P20] M. Antonello et al. (ICARUS Collaboration), "*Experimental observation of an extremely high electron lifetime with the ICARUS-T600 LAr-TPC*", Journal of Instrumentation, 9 (12), art. no. P12006 (2014). DOI: 10.1088/1748-0221/9/12/P12006.

[P21] M. Antonello et al. (ICARUS Collaboration), "*Operation and performance of the ICARUS T600 cryogenic plant at Gran Sasso underground Laboratory*", Journal of Instrumentation, 10 (12), art. no. P12004 (2015). DOI: 10.1088/1748-0221/10/12/P12004.

[P22] M. Antonello et al. (ICARUS Collaboration), *"Muon momentum measurement in ICARUS-T600 LAr-TPC via multiple scattering in few-GeV range*", Journal of Instrumentation, 12 (4), art. no. P04010 (2017). DOI: 10.1088/1748-0221/12/04/P04010.

References

[1] C. Rubbia, *The Liquid-Argon Time Projection Chamber: A new concept for neutrino detector*, CERN-EP-77-08 (1977).

[2] B. Baibussinov et al., Journal of Instrumentation **5** (2010) P12006.

[3] OPERA collaboration, T. Adam et al., arXiv:1109.4897v1[hep-ex] (2011).

[4] A.G. Cohen and S.L. Glashow, Phys. Rev. Lett. 107 (2011) 181803.

[5] F. Arneodo et al. (ICARUS Coll.), "The ICARUS Experiment: a second-generation Proton decay experiment and Neutrino Observatory at Gran Sasso Observatory", arXiv:hep-ex/0103008.

[6] A. Aguilar et al. [LSND Coll.], Phys. Rev. D 64, 112007 (2001).

[7] A. A. Aguilar-Arevalo et al. [MiniBooNE Coll.],PRL 110, 161801 (2013) and references therein.

[8] J. N. Abdurashitov et al. [SAGE Coll.], Phys. Rev. C 80, 015807 (2009).

[9] F. Kaether, W. Hampel, G. Heusser, J. Kiko, and T. Kirsten [GALLEX], Phys. Lett. B 685, 47 (2010) and references therein.

[10] G. Mention et al., Phys.Rev. D83 (2011) 073006 and references therein.

[11] C. Zhang, X. Quian, P. Vogel, Phys. Rev. D 87, 073018 (2013).

[12] A. Ferrari et al., CERN-2005-10, INFN/TC-05/11 (2005).

[13] Battistoni et al., AIP Conf. Proc. 896, 31-49, (2007).

[14] G. Battistoni et al. (FLUKA Coll.), in Proceedings of the 12thInternational Conference on nuclear reaction mechanisms, Varenna, Italy, June 15-19 (2009), p.307.

[15] http://proj-cngs.web.cern.ch/proj-cngs/ .

[16] R. Acciarri et al., arXiv:1503.01520 [physics.ins-det].

[17] www.stirlingcrogenics.com.